Proceedings of the CERN-BINP Workshop for Young Scientists in e^+e^- Colliders, Geneva, Switzerland, 22 – 25 August 2016, edited by V. Brancolini ans L. Linssen, CERN Proceedings, Vol. 1/2017, CERN-Proceedings-2017-001 (CERN, Geneva, 2017)

Study of the Conversion Decays of Omega Meson to π^0 Meson and e^+e^- Pair Using the CMD-3 Detector

R.R. Akhmetshin, A.N. Amirkhanov, A.V. Anisenkov, V.M. Aulchenko, V.S. Banzarov, N.S. Bashtovoy, A.E. Bondar, A.V. Bragin, S.I. Eidelman, D.A. Epifanov, L.B. Epshteyn, A.L. Erofeev, G.V. Fedotovich, S.E. Gayazov, A.A. Grebenuk, S.S. Gribanov, D.N. Grigoriev, F.V. Ignatov, V.L. Ivanov, S.V. Karpov, V.F. Kazanin, O.A. Kovalenko, A.A. Korobov, A.N. Kozyrev, E.A. Kozyrev, P.P. Krokovny, A.E. Kuzmenko[*]*, A.S. Kuzmin, I.B. Logashenko, P.A. Lukin, K.Y. Mikhailov, V.S. Okhapkin, Y.N. Pestov, A.S. Popov, G.P. Razuvaev, A.A. Ruban, N.M. Ryskulov, A.E. Ryzhenenkov, V.E. Shebalin, D.N. Shemyakin, B.A. Shwartz, A.L. Sibidanov, E.P. Solodov, V.M. Titov, A.A. Talyshev, A.I. Vorobiov, and Y.V. Yudin*
Budker Institute of Nuclear Physics, Novosibirsk, Russia

Abstract
The conversion decay $\omega \to \pi^0 e^+e^-$ was studied in the centre-of-mass energy range 760–840 MeV using about $8\,\mathrm{pb}^{-1}$ of data collected with the CMD-3 detector at the VEPP-2000 e^+e^- collider in Novosibirsk. The visible cross-section of the process $\omega \to \pi^0 e^+e^-$ was measured. The current status of the analysis is presented.

Keywords
Conversion decay; close tracks; vertex.

1 Introduction

The interest in the decay $\omega \to \pi^0 e^+e^-$ is related to the transition form factors of the ω meson that can be measured in this decay [1]. The precise value of the decay branching ratio can be useful for interpretation of experiments on quark–gluon plasma [2, 3]. This analysis is based on $8\,\mathrm{pb}^{-1}$ of data, which were collected in the centre-of-mass energy range 760–840 MeV by the CMD-3 detector. This data sample is twice as large as the sample previously used at the former CMD-2 detector.

The general purpose detector CMD-3 has been described in detail elsewhere [4]. The tracking system consists of the cylindrical drift chamber and double-layer multiwire proportional Z-chamber, both also used for the trigger. The tracking system is placed inside a thin superconducting solenoid with a field of 1.3 T. Electromagnetic calorimeters are place outside the solenoid: a LXe barrel calorimeter with a thickness of $5.4X_0$ and CsI crystals with a thickness of $8.1X_0$. An endcap calorimeter is made of BGO scintillation crystals, with a thickness of $13.4X_0$.

2 Data analysis

The decay $\omega \to \pi^0 e^+e^-$ has been studied using the π^0 dominant decay mode $\pi^0 \to \gamma\gamma$. It corresponds to a final state with two opposite charge particles and two photons. One of the significant resonant backgrounds comes from the $\omega \to \pi^+\pi^-\pi^0$ decay, which has the same topology as the final state and more than three orders of magnitude larger probability. Another source of resonant background is the $\omega \to \pi^0\gamma$ decay, followed by the Dalitz decay of the π^0 or γ-quantum conversion in the material in front of the drift chamber. The non-resonant background includes contributions from the following quantum electrodynamics (QED) processes with the same final state topology: $e^+e^- \to e^+e^-\gamma\gamma$, $e^+e^- \to 3\gamma$ followed by γ-quantum conversions, $e^+e^- \to e^+e^-\gamma$ with one background photon as well as a two-quantum annihilation followed by a γ-quantum conversion and one background photon in the calorimeters.

To select events of the process under study, we used the following criteria.

[*]Corresponding author.

https://doi.org/10.23727/CERN-Proceedings-2017-001.91

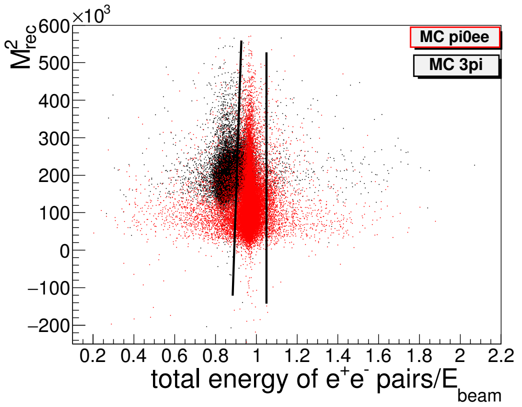

Fig. 1: Recoil mass of photon pairs versus total energy of electron–positron pairs, normalized to beam energy for Monte Carlo simulation of $\pi^0 e^+e^-$ (red dots) and $\pi^+\pi^-\pi^0$ (black dots). Black line shows selection cut.

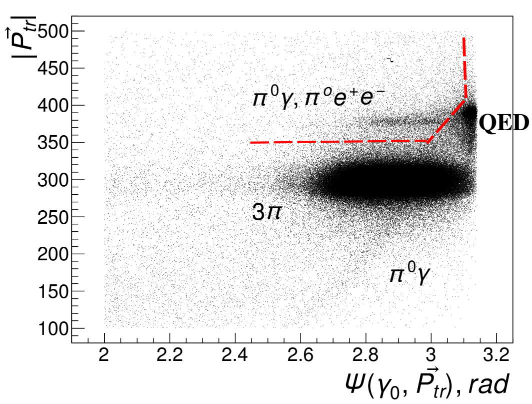

Fig. 2: Total momentum of charged particles P_{tr} versus angle between the most energetic photon and P_{tr}. The red line presents the selection cut.

- $N_\gamma \geq 2$ with energy 40 MeV $< E_{\gamma\,\max 0,1} < 2 \cdot E_{\mathrm{beam}}$ to suppress background photons in the calorimeters.
- The impact parameter of the tracks $\rho < 1$ cm and the Z-coordinate of the vertex $|Z_{\mathrm{vert}}| < 5$ cm to reject cosmic rays and beam background events.
- Two 'good' tracks in the drift chamber (with transverse moment $P^{\mathrm{tr}}_{1,2} > 40$ MeV/c and with polar angle $0.9 < \Theta_{1,2} < \pi - 0.9$).
- The opening angle between tracks $\Delta\psi < 1$ rad to suppress events of the $\omega \to \pi^+\pi^-\pi^0$ decay.
- Noncollinear tracks in the R–ϕ projection $|\pi - |\phi_1 - \phi_2|| > 0.15$.
- The angle between the total momentum of the tracks and each photon is greater than 1.5 rad to suppress QED events.
- The angle between photons is less than 1.6 rad to suppress events from the decay $\omega \to \pi^0\gamma$.
- The recoil mass of photon pairs, where it is understood that they originated from the π^0 decay $M^2_{\mathrm{rec}} = (2 \cdot E_{\mathrm{beam}})^2 - 4E_{\mathrm{beam}}E_{\pi^0} + m^2_{\pi^0}$, where $E_{\pi^0} = E_{\gamma,1} + E_{\gamma,2}$, and $E_{\gamma,i}$ is the energy of photon i in the calorimeter. The recoil mass of photon pairs is shown in Fig. 1. The black line in Fig. 1 presents the selection cut.
- The dependence of the total momentum of charged particles (P_{tr}) from the angle between the most energetic photon and P_{tr} is used to suppress $\omega \to \pi^+\pi^-\pi^0$ events as well as $\omega \to \pi^0\gamma$ events followed by the Dalitz decay of π^0. The red line in Fig. 2 is used for selection.
- The invariant mass of the electron–positron pair and the most energetic photon $M_{\mathrm{inv}}(e^+e^-\gamma_{\max 0})$ is less than $1.9 \cdot E_{\mathrm{beam}}$ to suppress $e^+e^- \to \gamma\gamma$ events followed by the conversion of the γ.

3 Separation of $\pi^0 e^+e^-$ and $\pi^0\gamma$ (with γ conversion on detector material)

The only difference between the $\pi^0 e^+e^-$ and $\pi^0\gamma$ with γ conversion on the detector material is that the vertex of tracks is shifted from the beam by 1.7–2 cm (vacuum tube) in the transverse plane. To analyse these events, we use $\gamma\gamma$ events, in which one γ is converted on the material. For separation, we use a neural network with input parameters:

- the angle between the tracks;
- The total momentum normalized to beam energy;

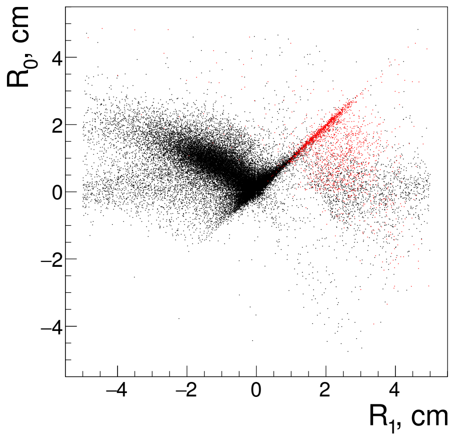

Fig. 3: Distance from beam point to first cross-point versus distance to second cross-point for Monte Carlo simulation of $\pi^0 e^+e^-$ (black dots) and $\gamma\gamma$ with photon conversion on material (red dots).

- the track momentum normalized to beam energy;
- the distance from the vertex to the centre of the beam. The sign of the distance is '+' when the angle between the beam point direction to a cross-point and the average momentum of the tracks is sharp and '$-$' otherwise. In the transverse plane, circles from tracks have two cross-points: the first is the vertex and the second is additional. These parameters are shown in Fig. 3.

The output parameter of the neural network determines the event type (signal ($\pi^0 e^+e^-$) or background (conversion γ on the detector material). Using this option to separate the events, we achieved the following efficiency of suppression: for $\pi^0\gamma - 84\%$ (for $\gamma\gamma - 90\%$), while we lost 2% of signal events.

4 Reconstruction efficiency of close tracks

Since Monte Carlo simulation does not completely describe the experiment, a correction $\varepsilon_{\Delta\psi}$ for a difference between the reconstruction efficiencies of close tracks in simulation and experiment was included. Its value was obtained using events of $\omega \to \pi^+\pi^-\pi^0$ decays followed by the conversion decay $\pi^0 \to e^+e^-\gamma$ with a similar $\Delta\psi$ distribution. $\varepsilon_{\Delta\psi}$ is calculated by averaging the integral in Eq. (1) for simulation events ($\omega \to \pi^0 e^+e^-$):

$$\varepsilon_{\Delta\psi} = \int \frac{\varepsilon^-_{\Delta\psi,\mathrm{exp}}(P^-_\perp)}{\varepsilon^-_{\Delta\psi,\mathrm{sim}}(P^-_\perp)} \cdot \frac{\varepsilon^+_{\Delta\psi,\mathrm{exp}}(P^+_\perp)}{\varepsilon^+_{\Delta\psi,\mathrm{sim}}(P^+_\perp)} f(P^-_\perp) f(P^+_\perp) \mathrm{d}P^-_\perp \mathrm{d}P^+_\perp \,, \tag{1}$$

where $\varepsilon^-_{\Delta\psi,\mathrm{exp}}(P^-_\perp)$ is the efficiency of track reconstruction depending on the transverse momentum (for e^- or e^+, and for simulation or experiment) (see Fig. 4):

$$\varepsilon_{\Delta\psi} = 0.970 \pm 0.008 \pm 0.020 \,. \tag{2}$$

5 Results

The detection efficiency, $\varepsilon^{\pi^0 e^+e^-}_{\mathrm{det}} = 23\%$, was determined using Monte Carlo simulation based on the GEANT4 [5].

The number of signal and background events has been obtained from a fit of the $\gamma\gamma$ invariant mass distribution at each energy point. The signal was described by a two-Gauss function, the background shape was described by a Gauss function and a constant. The shapes of the signal and background curve

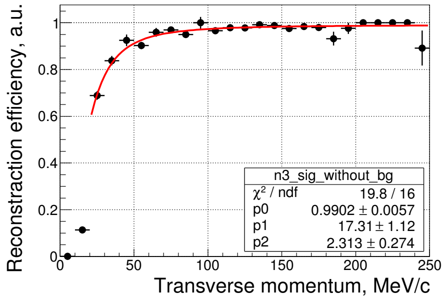

Fig. 4: Efficiency of track reconstruction versus transverse momentum for e^- for experimental data

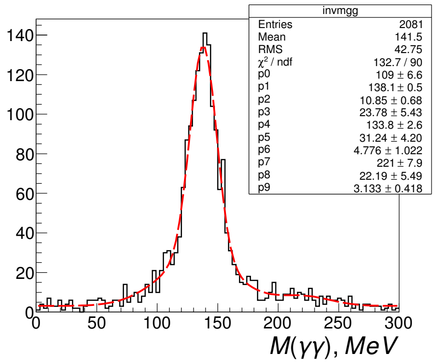

Fig. 5: Invariant mass of $\gamma\gamma$ for experimental data in energy range 760–840 MeV

Table 1: Results from current and other experiments

Experiment	Br($\omega \to \pi^0 e^+ e^-$)	Events	Data, pb^{-1}
ND [6]	$(5.9 \pm 1.9) \cdot 10^{-4}$	43	
CMD-2 [7]	$(8.19 \pm 0.71 \pm 0.62) \cdot 10^{-4}$	230	3.3
SND [8]	$(7.61 \pm 0.53 \pm 0.64) \cdot 10^{-4}$	613	9.8
CMD-3 (preliminarily)[a]	$(8.81 \pm 0.35) \cdot 10^{-4}$ (stat.)	1380	8

[a] The trigger efficiency and the contributions of $\omega \to \pi^+\pi^-\pi^0$, $\omega \to \pi^0\gamma$ were not taken into account.

were fixed from the fit of experimental data in the energy range 760–820 MeV (see Fig. 5), so the varying parameters at each energy point were the number of signal and background events. These values were used to determine the visible cross-section of the signal (see Fig. 6), using Eq. (3) and background events (see Fig. 7), using Eq. (4):

$$\sigma_{\text{vis}} = \frac{N_{\text{sig,i}}}{L_i(1+\delta_i) \cdot \varepsilon_{\text{det}} \cdot \varepsilon_{\Delta\psi} \cdot \text{Br}(\pi^0 \to \gamma\gamma)}, \tag{3}$$

$$\sigma_{\text{vis bg}} = \frac{N_{\text{bg,i}}}{L_i \cdot \varepsilon_{\text{det}}}. \tag{4}$$

The current value of Br($\omega \to \pi^0 e^+ e^-$) (the trigger efficiency and the contributions of $\omega \to \pi^+\pi^-\pi^0$, $\omega \to \pi^0\gamma$ were not taken into account) obtained and the most important results from other experiments are presented in Table 1.

The study of the trigger efficiency, a test of the method of determining $\pi^0\gamma/\pi^0 e^+ e^-$, and separa-

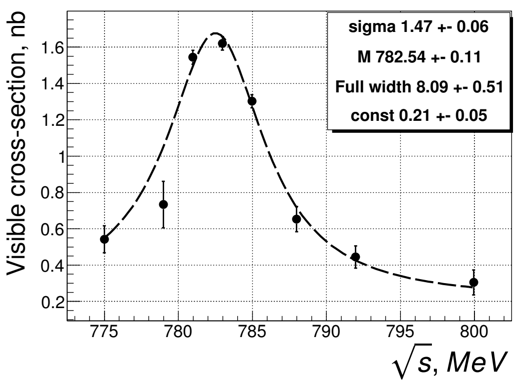

Fig. 6: Visible cross-section of signal process, fitted with Breit–Wigner distribution.

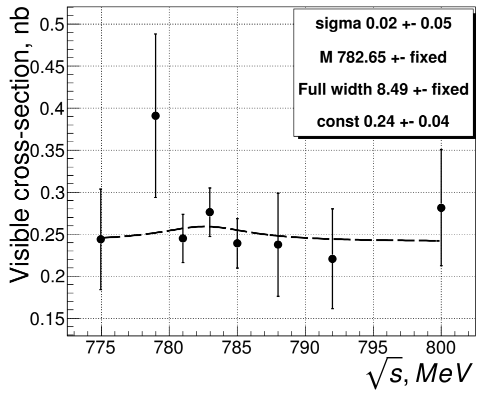

Fig. 7: Visible cross-section of background events, fitted with Breit–Wigner distribution.

tion using QED events and analysis of systematics are included in our plans for the future. We also plan to measure the transition form factor of the ω meson.

References

[1] L. Landsberg, *Phys. Rep.* **128** (1985) 301. `https://doi.org/10.1016/0370-1573(85)90129-2`

[2] E.V. Shuryak, *Phys. Lett.* **B 78** (1978) 150. `https://doi.org/10.1016/0370-2693(78)90370-2`

[3] D. Adamova *et al.*, *Phys. Rev. Lett.* **91** (2003) 042301. `https://doi.org/10.1103/PhysRevLett.91.042301`

[4] B.I. Khazin *et al.* (CMD-3 Collaboration), *Nucl. Phys. B Proc. Suppl.* **181–182** (2008) 376. `https://doi.org/10.1016/j.nuclphysbps.2008.09.068`

[5] S. Agostinelli *et al.* (GEANT4 Collaboration), *Nucl. Instrum. Methods Phys. Res. A* **506** (2003) 250. `https://doi.org/10.1016/S0168-9002(03)01368-8`

[6] S.I. Dolinsky *et al.*, *Sov. J. Nucl. Phys.* **48** (1988) 277.

[7] R.R. Akhmetshin *et al.* (CMD-2 Collaboration), *Phys. Lett.* **B613** (2005) 29. `https://doi.org/10.1016/j.physletb.2005.03.019`

[8] M.N. Achasov *et al.* (SND Collaboration), *J. Exp. Theor. Phys.* **107** (2008) 61.